

Abnormally high HIP1 expression is associated with metastatic behaviors and poor prognosis in ESCC

YING SUN*, YONGAN ZHOU*, JINGHUA XIA, MIAOMIAO WEN, XUEJIAO WANG,
JIAO ZHANG, YANNING ZHANG, ZHIPEI ZHANG and TAO JIANG

Department of Thoracic Surgery, Second Affiliated Hospital of
Air Force Medical University, Xi'an, Shaanxi 710038, P.R. China

Received June 8, 2020; Accepted October 19, 2020

DOI: 10.3892/ol.2020.12340

Abstract. Huntingtin interacting protein 1 (HIP1) is overexpressed in several human malignancies. However, the biological function of HIP1 in esophageal squamous cell carcinoma (ESCC), and its effect on the prognosis of patients remain unclear. The present study aimed to investigate HIP1 expression in ESCC via immunohistochemistry, reverse transcription-quantitative PCR and western blot analyses. The association between HIP1 expression and the clinicopathological characteristics of 173 patients with ESCC was statistically analyzed. The effect of HIP1 expression on patient prognosis was assessed via Kaplan-Meier and Cox regression analyses. Lentivirus-delivered RNA interfering technique was used to overexpress and downregulate HIP1 expression in ESCC cell lines. The results demonstrated that HIP1 expression was significantly higher in ESCC tissues compared with adjacent normal tissues, and HIP1 expression was associated with histological differentiation, tumor-node-metastasis stage and lymph node metastasis. Furthermore, the overall survival time of patients with high HIP1 expression was significantly shorter than those with low HIP1 expression. Cellular mobility demonstrated that overexpressing HIP1 increased ESCC proliferation, migration and invasion, whereas silencing HIP1 decreased ESCC proliferation, migration and invasion. Furthermore, overexpressing HIP1 induced ESCC cells to enter the S and G2 phases from the G1 phase, whereas HIP1 knockdown arrested the cell cycle in the G1 phase. Taken together, the results of the present study suggest that HIP1 is associated with proliferation and metastatic

behaviors in ESCC, and thus may be used as a potential prognostic indicator for patients with ESCC.

Introduction

Molecular targeted therapy is considered a novel treatment method following surgery, radiotherapy and chemotherapy (1). Molecular targeted drugs, such as gefitinib (2), lapatinib (3), pazopanib (4), have been successfully applied for the treatment of lung, breast and colon cancers. However, there is currently a lack of effective targeted drugs for esophageal cancer. Thus, further studies are required to understand the tumorigenesis and identify therapeutic targets for esophageal cancer.

Huntingtin interacting protein 1 (HIP1) is a protein associated with Huntington's disease (5). HIP1, as an endocytic oncoprotein, participates in clathrin-mediated vesicle trafficking (6,7). Previous studies have demonstrated the involvement of HIP1 in tumorigenesis (8,9). For example, Marghalani *et al* (10) demonstrated that HIP1 contributes to the pathological diagnosis of Merkel cell carcinoma. Furthermore, Rao *et al* (11) reported that HIP1 is overexpressed in prostate and colon cancers, whereby its high expression levels promote cancer cell survival. Thus, it was hypothesized that HIP1 may be a novel oncogene in malignant tumor. However, the role of HIP1 in esophageal squamous cell carcinoma (ESCC) remains unclear. Thus, the present study aimed to investigate HIP1 expression in 173 ESCC tissues via immunohistochemical staining. In addition, the association between HIP1 expression and the clinicopathological characteristics of patients with ESCC was statistically analyzed. HIP1 was overexpressed and downregulated in ESCC cell lines, and its biological functions were investigated *in vitro*.

The results of the present study demonstrated that HIP1 expression was higher in ESCC tissues compared with adjacent normal tissues. Furthermore, high HIP1 expression was associated with promoting ESCC metastasis, while low HIP1 expression inhibited ESCC metastasis. Taken together, these results suggest that HIP1 may be a marker to predict the metastasis of patients with ESCC.

Materials and methods

Patients and tissue samples. A total of 178 paraffin-embedded ESCC tissues were randomly selected from the biological sample

Correspondence to: Professor Tao Jiang or Professor Zhipei Zhang, Department of Thoracic Surgery, Second Affiliated Hospital of Air Force Medical University, 569 Xinsi Road, Xi'an, Shaanxi 710038, P.R. China
E-mail: jiangtaotd@163.com
E-mail: zzpzyy@fmmu.edu.cn

*Contributed equally

Key words: huntingtin interacting protein 1, metastasis, prognosis, esophageal squamous cell carcinoma

bank at the Department of Thoracic Surgery, Second Affiliated Hospital of Air Force Medical University (Xi'an, China), between December 2006 and February 2013. Patients who received preoperative chemotherapy, radiotherapy or other treatments were excluded from the present study. Among the 178 patients, 173 patients were confirmed ESCC (97.2%), and five patients were confirmed esophagus adeno cancer (EAC; 2.8%). Considering the small number of specimens, patients with EAC were also excluded from the present study. Among 173 patients, there were 139 men and 34 women (median age, 60 years; age range 41-79 years). Patient information, including age and sex were collected from the medical records. The last follow-up was on June 12, 2018, with a median follow-up period of 38 months (1-145 months). The present study was approved by the Regional Ethics Committee for Clinical Research of the Air Force Military Medical University (Xi'an, China; approval no. TDLL-201712-22). Written informed consent was provided by all patients prior to the study start for use of their medical records and tissue specimens for research purposes.

Cell culture. The ESCC cell lines (EC109, Kyse30, TE-10 and TE-11) were preserved at the Department of Thoracic Surgery, Second Affiliated Hospital of Air Force Medical University (Xi'an, China), while the human esophageal epithelial cell line (HEEpiC) was purchased from the American Type Culture Collection. All cells were maintained in RPMI-1640 medium (HyClone; GE Healthcare Life Sciences) supplemented with 10% fetal bovine serum (FBS, Gibco; Thermo Fisher Scientific, Inc.) and 1% penicillin/streptomycin (cat. no. C0222, Beyotime Institute of Biotechnology), at 37°C in 5% CO₂.

Immunohistochemistry (IHC). Tumor tissue samples were fixed with 10% formaldehyde for 48 h at room temperature and embedded in paraffin. Paraffin-embedded tissue samples were cut into 4- μ m-thick sections. Tissue sections were dewaxed using xylene, digested with urea for 30 min and incubated with 3% hydrogen peroxide for 30 min to inhibit endogenous peroxidase activity at room temperature. Subsequently, the tissue sections were repaired for 20 min (750 W for 5 min and 450 W for 15 min) using a microwave and cooled in citric acid buffer (pH 6.0). Tissue sections were blocked with 5% goat serum for 30 min and washed three times with PBS solution (5 min each time) at room temperature. The sections were incubated with HIP1 primary antibody (1:80; cat. no. 22231-1-AP; ProteinTech Group, Inc.) overnight at 4°C. Following the primary incubation, tissue sections were incubated with contents of the EnVision™ Detection kit (cat. no. CW20355, Kangwei, <http://cwbiotech.bioon.com.cn/>) at 37°C for 45 min, according to the manufacturer's instructions (12). The sections were subsequently counterstained with hematoxylin for 90 secs and treated with hydrochloric acid alcohol differentiation fluid for 7 sec at room temperature.

Evaluation of IHC staining. Following IHC staining, tissue sections were observed in five randomly selected fields under a fluorescence microscope (Leica Microsystems GmbH, DM4000B; magnification, x200). The total immunostaining score was calculated as the product of the proportion score and the intensity score (13). The proportion score represented the estimated fraction of positively stained tumor cells, as follows: 0, 0-5%; 1, 6-25%; 2, 26-50%; 3, 51-75% and 4, 76-100%. The

intensity score represented the estimated staining intensity, as follows: 0, negative; 1, weak; 2, moderate and 3, strong. These scores were measured according to the result of the degree multiplied by the score of the staining intensity, as follows: 0, 0; 1+, 1-4; 2+, 5-8 and 3+, 9-12. A score of 0 was considered negative, whereas scores 1+ to 3+ were considered positive. Thus, the total score ranged from 0-12.

Reverse transcription quantitative (RT-q)PCR. Total RNA was extracted from tissue samples and cell lines using TRIzol® reagent (Invitrogen; Thermo Fisher Scientific, Inc.), according to the manufacturer's protocol. Total RNA was reverse transcribed into cDNA using the Thermo scientific Revert Aid First Strand cDNA Synthesis kit (100rxns, Thermo Fisher Scientific, Inc.). qPCR was subsequently performed using the SYBR Green Premix Ex Taq II kit (cat. no. CW0957M; Kangwei, <http://cwbiotech.bioon.com.cn/>). Relative expression levels were calculated using the 2^{- $\Delta\Delta C_q$} method (14) and normalized to the internal reference gene β -actin.

The following primer sequences were used for qPCR: HIP1 forward, 5'-GTTGTGGCCTCAACCATT-3' and reverse, 5'-ACCACTTCTTGCAGTGTAG-3'; and β -actin forward, 5'-CTCCATCCTGGCCTCGCTGT-3' and reverse, 5'-GCTGTCACCTTCACCGTTCC-3'. Relative expression levels were normalized to the internal reference gene β -actin.

Western blotting. Total protein was extracted from tissues and cells using RIPA lysate (cat. no. P0013; Beyotime Institute of Biotechnology). Total protein was quantified using the BCA Protein Assay kit (cat. no. 23227, Pierce; Thermo Fisher Scientific, Inc.). The extracted protein was mixed with the loading buffer (10x, cat. no. CW0027A; CWBio) and heated at 65°C for 30 min. The proteins (30 μ g) were separated by SDS-PAGE (5% concentrated glue and 12% separated glue). Subsequently, the proteins were transferred onto the polyvinylidene fluoride membranes (Beijing Solarbio Science & Technology Co., Ltd.) via electroblotting (Bio-Rad Laboratories, Inc.). Membranes were blocked with 5% skim milk powder, which was dissolved in TBST for 3 h at room temperature, and subsequently incubated with HIP1 primary antibody (cat. no. 22231-1-AP, monoclonal antibody, 1:1,000, ProteinTech Group, Inc.) and β -actin (cat. no. CW0097, polyclonal antibody, 1:2,500, CWBio) diluted with WB Antibody Diluent (P0023A; Beyotime Institute of Biotechnology) overnight at 4°C. Following the primary incubation, the membranes were incubated with secondary antibody (1:5,000; cat. no. EK020; Zhuangzhi Bio, <http://www.zhuangzhibio.com>) diluted with WB Secondary Antibody Diluent (cat. no. P0023A; Beyotime Institute of Biotechnology) at room temperature for 35 min. Membranes were washed six times with TBST, and protein bands were detected using the Millipore chromogenic kit (cat. no. WBKLS0500; Millipore). Relative quantitative analysis was performed using the GelDox XR system (Bio-Rad Laboratories, Inc.) (15).

Lentiviral construction of stable cell lines with overexpressed or downregulated HIP1 and cell transfection. As demonstrated in Fig. 1E and F, HIP1 mRNA and protein expression levels are higher in EC109 cells compared with TE-10 cells, and lower in Kyser 0 cells compared with TE-11 cells. Thus,

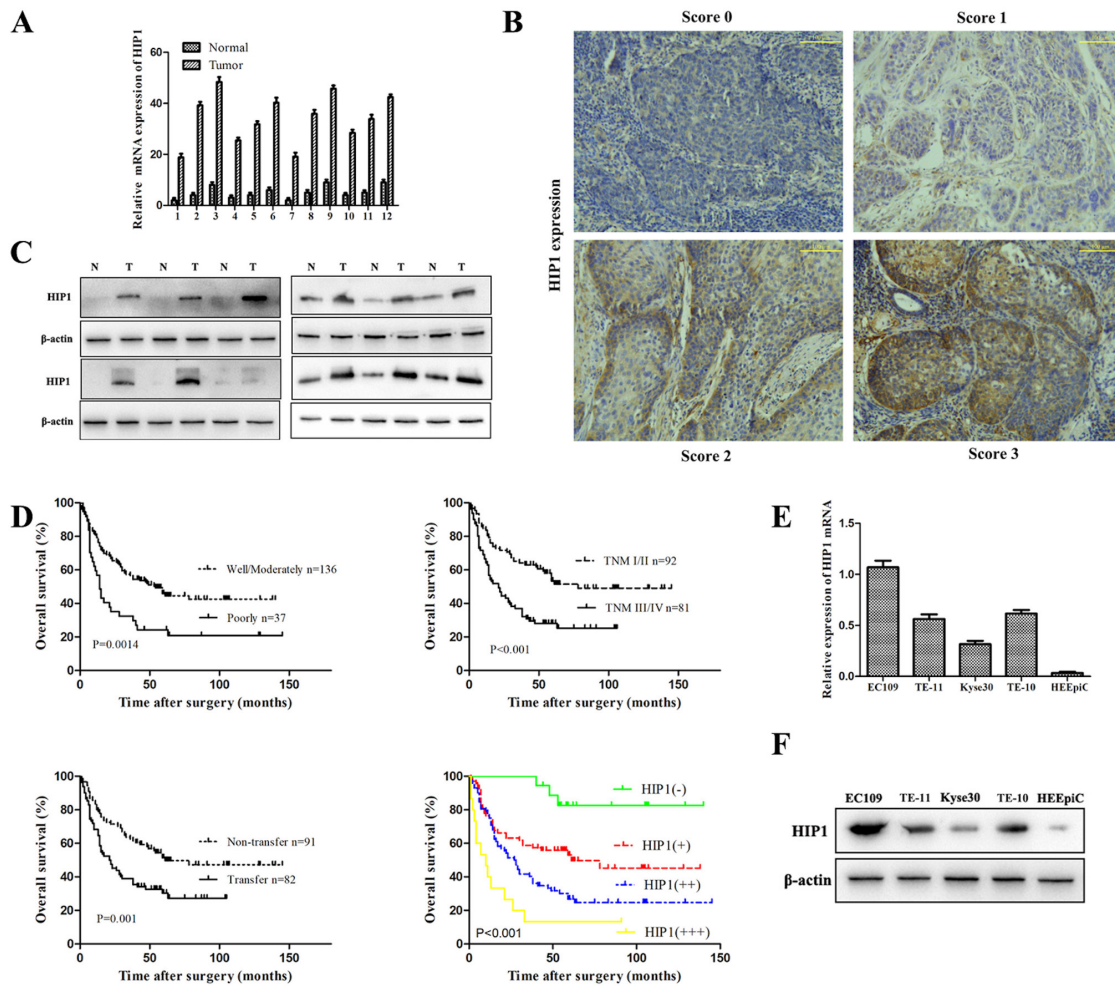


Figure 1. HIP1 is highly expressed in human ESCC and predicts a poor prognosis. (A) Reverse transcription-quantitative PCR analysis demonstrated that HIP1 mRNA expression levels were higher in ESCC tumor tissues compared with paracancerous tissues. (B) HIP1 expression in ESCC clinical specimens were divided into four groups (scores 0-3) by immunohistochemistry (magnification, $\times 200$). (C) Western blot analysis demonstrated that HIP1 protein expression levels were higher in ESCC tumor tissues compared with paracancerous tissues, and β -actin was used as the internal control. (D) Malignant differentiation (poor), late TNM stages (III-IV), transferred lymph node and high HIP1 expression were significantly associated with poor overall survival in patients with ESCC. (E) HIP1 mRNA expression levels were higher in ESCC cells compared with normal HEEpIC cells. (F) HIP1 protein expression levels were higher in ESCC cells compared with normal HEEpIC cells, and β -actin was used as the internal control. Data are presented as the mean \pm standard deviation. HIP1, huntingtin interacting protein 1; ESCC, esophageal squamous cell carcinoma; T, tumor; N, normal; TNM, tumor-node-metastasis; HEEpIC, human esophageal epithelial cell line.

EC109 was selected as the cell line where lentivirus interfered with the expression of the HIP1 gene, and Kyse30 was selected as the cell line that promoted the expression of the HIP1 gene.

To stably overexpress (OE) the HIP1 gene, Kyse30 cells were infected with a lentivirus vector encoding the full-length sequence of human HIP1 gene. The untargeted sequence was used as OE-control group. Untreated cells were used as the control group. When the infection efficiency of cells treated with lentivirus green fluorescent protein (GFP) reached 80%, and the results of RT-qPCR and western blotting found that significantly improving expressions of HIP1 mRNA and protein, the overexpression was considered successful.

EC109 cells were infected with hU6-MCS-CMV-EGFP-lentivirus or an empty lentiviral control vector (Shanghai GeneChem Co., Ltd.) to inhibit HIP1 gene expression (Genebank no. 3092). The short hairpin (sh)RNA HIP1 sequences were as follows: #1, 5'-AAGCTATTCAGGTGTCAT-3'; #2, 5'-TTCAATTCAACAGTCAAA-3'; and #3, 5'-TCTTCCAAACAGTATTCAA-3', and the shRNA control sequence was as follows: 5'-TTCTCCGAACGTGTCACGT-3'.

The untargeted sequence was used as the shRNA-control group, and untreated cells were used as the control group. When the infection efficiency of cells treated with lentivirus green fluorescent protein (GFP) reached 80%, and the results of RT-qPCR and western blot analyses demonstrated significant inhibition of HIP1 mRNA and protein levels, then the lentivirus interference succeeded.

MTT assay. After 6 days of lentivirus vector overexpression or shRNA infection, the treated cells were seeded into 96-well plates at a density of 4×10^3 cells/well. Cell viability was measured at days 1, 2, 3, 4, 5 and 6 following incubation at 37°C in 5% CO_2 . A total of 20 μl MTT reagent (5 mg/ml, dissolved in PBS; Sigma-Aldrich; Merck KGaA) was added into each well and incubated at 37°C for 4 h. Following the MTT incubation, the purple formazan crystals were dissolved using 150 μl dimethyl sulfoxide and cell viability was subsequently analyzed at a wavelength of 570 nm using an ELISA detector (Thermo Fisher Scientific, Inc.), and the growth curve was plotted according to the OD value (15).

Cell cycle analysis. The effect of HIP1 expression on ESCC cell cycle distribution was assessed via flow cytometry. Flow cytometric analysis was performed as previously described (15).

Wound healing assay. The wound healing assay was performed as previously described (16). Briefly, both transfected and untreated Kyse30 and EC109 cells were harvested and seeded into 6-well plates at a density of 5×10^5 cells/well, 5 days post-lentiviral vector overexpression or shRNA infection. Cells were incubated overnight at 37°C in 5% CO₂ until they reached 80% confluence, and the monolayer was subsequently scratched using a 200 μ l pipette tip. The debris was removed and fresh serum-free RPMI-1640 medium (HyClone; GE Healthcare Life Sciences) was added to the wells. Cells were captured at 0, 24 and 48 h using a fluorescence microscope (Zeiss, AXIOVERT 40C; magnification, x200). Cell migration was analyzed using ImageJ software (version 1.48u; National Institutes of Health) at three different sites from each wound area of scratch, at each time point. The percentage change in migration was determined by comparison of the differences in wound width.

Migration and invasion assays. The migration and invasion assays were performed *in vitro* as previously described (8) using 8 μ m pore size Transwell chambers (Corning, Inc.), according to the manufacturer's protocol. For the invasion assay, Matrigel (5 mg/ml; Corning, Inc.) was diluted in 1 mg/ml ice-cold RPMI-1640 medium supplemented with 10% FBS. An aliquot of 200 μ l diluted Matrigel was added to the upper Transwell chambers and incubated for 4 h at 37°C. A total of 1×10^5 transfected and untreated Kyse30 and EC109 cells were plated in the upper chambers in 400 μ l RPMI-1640 medium (HyClone; GE Healthcare Life Sciences) without FBS. RPMI-1640 medium (600 μ l) supplemented with 10% FBS was plated in the lower chambers as a chemo attractant. Following incubation for 48 h at 37°C, the non-invasive cells in the upper chambers were carefully removed using a cotton swab, while the invasive cells in the lower chambers were fixed in dehydrated alcohol for 30 min at room temperature and subsequently stained with 4 mg/ml crystal violet for 10 min at room temperature. Stained cells were counted in five randomly selected fields using a fluorescence microscope (magnification, x200).

Statistical analysis. Statistical analysis was performed using SPSS 18.0 software (SPSS, Inc.). Data are presented as the mean \pm standard deviation. All experiments were performed in triplicate. As the data were not normally distributed, non-parametric tests were used in the present study. The difference in HIP1 expression among three or more groups was assessed using the Kruskal-Wallis H and Mann-Whitney U tests. Survival analysis was performed using the Kaplan-Meier method, and the Cox proportional hazards model was used for multivariate analysis. $P < 0.05$ was considered to indicate a statistically significant difference.

Results

Patient characteristics. The clinicopathological data of 173 patients with ESCC are presented in Table I. Among these patients, 139 were men and 34 were women, with a

Table I. Patient characteristics (n=173).

Characteristic	Number of cases, n	%
Age, years		
Median	60	
Range	41-79	
Sex		
Male	139	80.3
Female	34	19.7
Smoking history		
Smoker	92	53.2
Non-smoker	81	46.8
Pathological type		
Squamous cell carcinoma	168	97.1
Adenocarcinoma	5	2.9
Differentiation		
Well	37	21.4
Moderate	99	57.2
Poor	37	21.4
TNM stage		
I-II	92	53.2
III-IV	81	46.8
Primary tumor size, cm		
≤ 4	91	52.6
> 4	82	47.4
Lymph node metastasis		
Yes	82	47.4
No	91	52.6
TNM, tumor-node-metastasis.		

median age of 60 years (age range, 41-79 years). Among the 173 patients, 37 cases were highly differentiated (21.4%), 99 cases were moderately differentiated (57.2%) and 37 cases were poorly differentiated (21.4%). With regards to the tumor-node-metastasis (TNM) stage, 92 cases were classified as stages I-II (53.2%), while 81 cases were classified as stages III-IV (46.8%). All tumors were staged according to the pathological tumor/node/metastasis (p-TNM) classification (8th edition) of the International Union against Cancer (17).

HIP1 is highly expressed in human ESCC tissues and cell lines, and predicts a poor prognosis. HIP1 mRNA expression was significantly higher in ESCC tissues compared with adjacent normal tissues (Fig. 1A). IHC analysis demonstrated that there were 155 positive results of HIP1 in ESCC tissues (89.6%, 155/173), which was higher than that of HIP1 in adjacent normal tissues (23.1%, 40/173). The ESCC staining results were sub-divided into four groups: HIP1 negative group (score 0), low HIP1 expression group (score 1), moderate HIP1 expression group (score 2) and high HIP1 expression group (score 3). The HIP1 positive rate in the ESCC tissues of the moderate and high groups (50.3%) was higher than that in the low group (39.3%) (Fig. 1B). Furthermore, HIP1 protein

Table II. Association between HIP1 expression and the clinicopathological characteristics of patients with esophageal squamous cell carcinoma.

Characteristic	Number of patients, n	HIP1 expression				P-value
		-	+	++	+++	
Sex						0.281
Male	139	17	48	60	14	
Female	34	1	20	12	1	
Age, years						0.427
≤60	78	5	33	32	8	
>60	95	13	35	40	7	
Smoking history						0.911
Smoker	92	14	32	34	12	
Non-smoker	81	4	36	38	3	
Primary tumor size, cm						0.140
≤4	91	8	33	40	10	
>4	82	10	35	32	5	
Differentiation						<0.001
Well	37	7	22	8	0	
Moderate	99	6	34	48	11	
Poor	37	5	12	16	4	
TNM stage						<0.001
I-II	92	12	46	30	4	
III-IV	81	6	22	42	11	
Lymph node metastasis						<0.001
Yes	82	4	26	40	12	
No	91	14	42	32	3	

HIP1, huntingtin interacting protein 1; TNM, tumor-node-metastasis.

expression was significantly higher in ESCC tissues compared with the adjacent normal tissues (Fig. 1C).

The results demonstrated that high positive HIP1 expression was significantly associated with moderate and poor differentiation, TNM stages III-IV and lymph node metastasis, while low positive HIP1 expression was significantly associated with well differentiation ($P<0.001$), TNM stages I-II ($P<0.001$) and lymph node non-metastasis ($P<0.001$) (Table II). Kaplan-Meier survival analysis demonstrated that differentiation ($P=0.001$), TNM stages ($P<0.001$), lymph node metastasis ($P=0.001$) and HIP1 expression ($P<0.001$) were all significantly associated with the overall survival (OS) time of patients with ESCC (Fig. 1D and Table III). Cox regression analysis indicated that differentiation ($P=0.037$), TNM stages ($P=0.014$) and HIP1 expression ($P=0.001$) were significant prognostic influences for OS (Table IV).

Higher HIP1 mRNA levels were detected in ESCC cell lines compared with HEEpiC cells. With regards to the ESCC cell lines, HIP1 mRNA expression was higher in EC109 and TE-10 cells and lower in Kyse30 and TE-11 cells (Fig. 1E). HIP1 protein expression levels were significantly higher in ESCC cells compared with HEEpiC cells. With regards to the ESCC cell lines, HIP1 protein expression was higher in EC109 and T10 cells, and lower in Kyse30 and T11 cells (Fig. 1F).

Silencing HIP1 expression by lentivirus-delivered RNA interfering. To further investigate the underlying molecular mechanism of HIP1 in ESCC, EC109 cells were infected with shRNA-HIP1 (#1, #2 and #3) and shRNA-control. The infection efficiency of green fluorescent protein (GFP) in EC109 cells infected with shRNA-HIP1-3 was 80~85% after 3 days of infection, at a multiplicity of infection (MOI) of 10 (Fig. 2A). After 3 days of interfering, RT-qPCR and western blot analyses were performed to determine the knockdown efficiency, respectively. The results demonstrated that HIP1 mRNA and protein expressions levels were significantly inhibited in cells transfected with shRNA-HIP1-3 ($P<0.05$; Fig. 2B and C), and moderately decreased by the other two shRNAs (shRNA-HIP1-1 and shRNA-HIP1-2 compared with the shRNA-control group and control group. Thus, shRNA-HIP1-3 was selected for further lentivirus-delivered RNA interfering experiments. The successful establishment of a HIP1 gene silencing lentivirus provided a useful tool for further investigating the function of HIP1 in ESCC cell lines.

HIP1 knockdown significantly suppresses ESCC cell proliferation, migration and invasion. The results of the MTT assay demonstrated that shRNA-HIP1 cells proliferated at a slower rate compared with the shRNA-control and control group cells, whereby the difference was statistically significant from day 4 (Fig. 3A). The results of the

Table III. Kaplan-Meier survival analysis of variables affecting survival in patients with esophageal squamous cell carcinoma.

Variable	Number of patients, n	Mean overall survival, months	95% CI, months	P-value
Total, n	173	68.600	59.052-78.148	
Age, years				
≤60	78	65.663	52.122-79.205	0.685
>60	95	69.873	56.979-82.767	
Sex				
Male	139	63.366	53.302-73.429	0.175
Female	34	83.054	60.842-105.265	
Smoking history				
Never	81	69.335	55.276-83.395	0.794
Ever	92	65.363	53.097-77.630	
Differentiation				
Well + moderate	136	73.469	63.027-83.910	0.001
Poor	37	42.961	25.411-60.512	
TNM stage				
I-II	92	85.222	72.178-98.267	<0.001
III-IV	81	39.948	30.924-48.973	
Lymph node metastasis				
No	91	82.656	69.632-95.679	0.001
Yes	82	41.865	32.663-51.067	
HIP1 expression				
--+	86	86.883	73.578-100.187	<0.001
++-+++	87	48.335	36.683-59.987	

CI, confidence interval; TNM, tumor-node-metastasis; HIP1, huntingtin interacting protein 1.

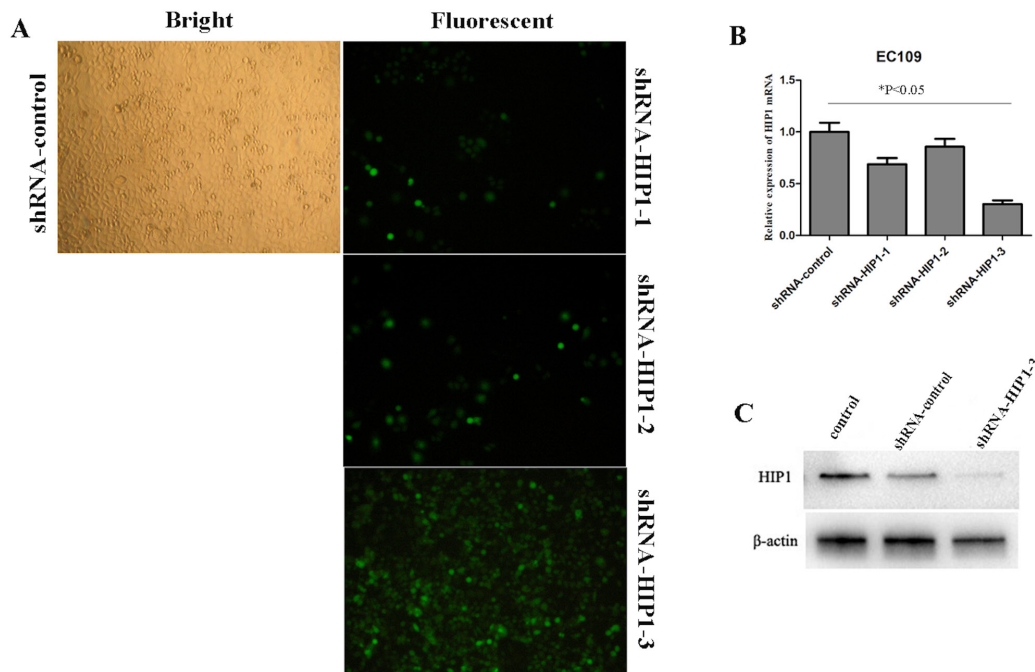


Figure 2. HIP1 expression is significantly inhibited in EC109 cells transfected with shRNA-HIP1. (A) Micrograph of EC109 cells infected with shRNA-HIP1 for 3 days in bright and fluorescent fields (magnification, 100x). The results demonstrated that >80% of cells expressed green fluorescent protein in shRNA-HIP1-3. (B) Reverse transcription-quantitative PCR analysis demonstrated that HIP1 mRNA expression was inhibited in cells transfected with shRNA-HIP1-1 and shRNA-HIP1-2 compared with the shRNA-control and control groups, while HIP1 mRNA expression was significantly inhibited in cells transfected with shRNA-HIP1-3. (C) Western blot analysis demonstrated that HIP1 protein expression in cells transfected with shRNA-HIP1-3 was remarkably lower compared with the of shRNA-control and control cells. *P<0.05. HIP1, huntingtin interacting protein 1; sh, short hairpin.

Table IV. Multivariate analysis for overall survival according to Cox proportional hazards model.

Variable	Category	Multivariate analysis	
		HR (95% CI)	P-Value
Differentiation	Poor/well + moderate	1.603 (1.030-2.496)	0.037
TNM stage	I-II/III-IV	0.593 (0.390-0.901)	0.014
HIP1 expression	--+/+++----	2.004 (1.310-3.067)	0.001

TNM, tumor-node-metastasis; HIP1, huntingtin interacting protein 1; HR, hazard ratio; CI, confidence interval.

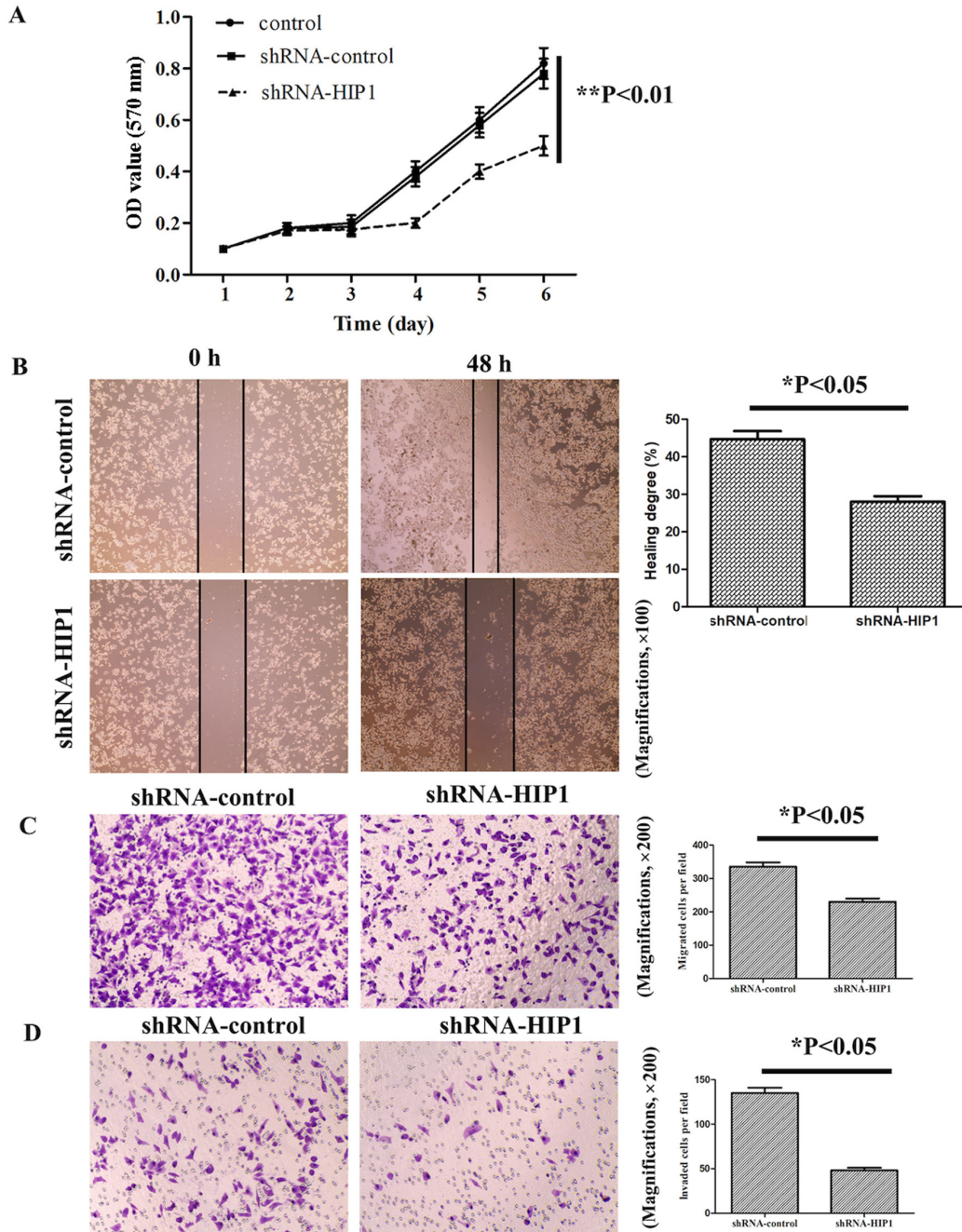


Figure 3. HIP1 knockdown significantly suppresses esophageal squamous cell carcinoma cell proliferation, migration and invasion. (A) The results of the MTT assay demonstrated that shRNA-HIP1 cells proliferated at a slower rate, in a time-dependent manner, compared with the shRNA-control and control cells. (B) The wound healing and (C) Transwell migration assays demonstrated that HIP1 knockdown inhibited the migratory ability of EC109 cells (magnifications, x100 and x200, respectively). (D) The Transwell invasive assay demonstrated that HIP1 knockdown inhibited the invasive ability of EC109 cells (magnification, x200). *P<0.05, **P<0.01. HIP1, huntingtin interacting protein 1; sh, short hairpin; OD, optical density.

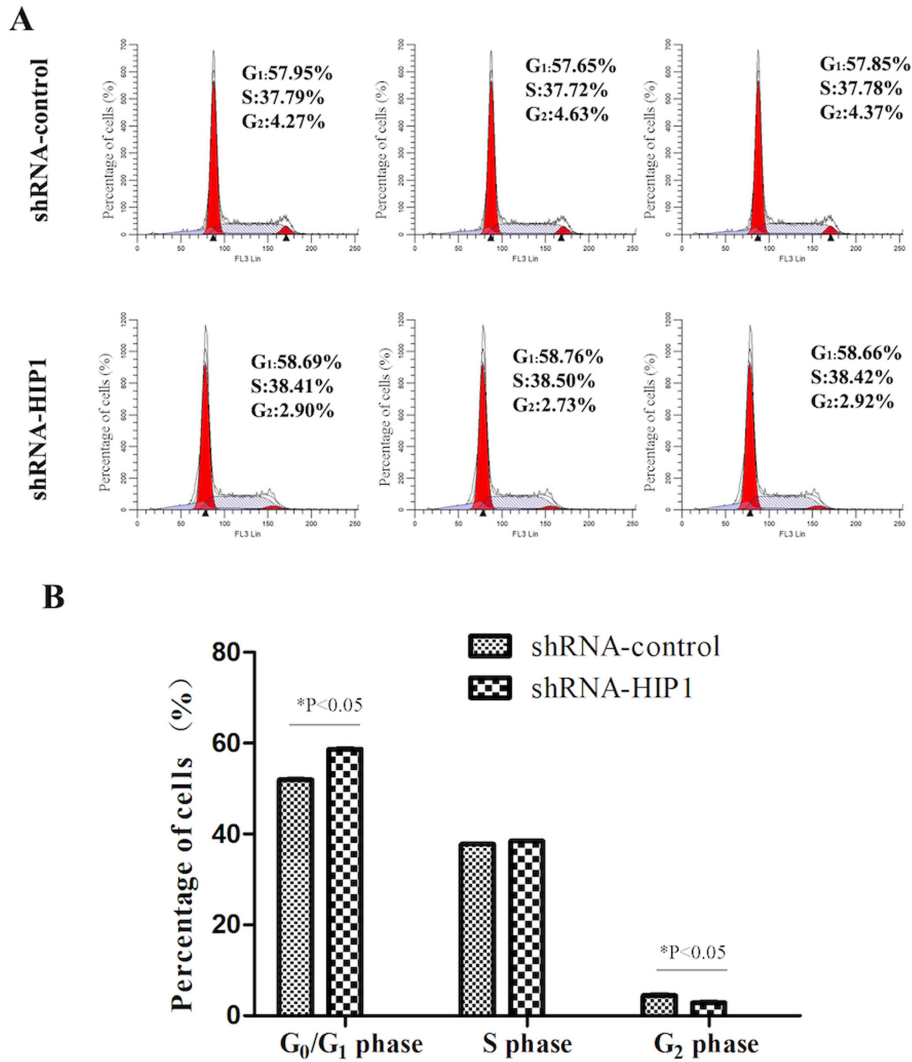


Figure 4. Percentage of HIP1 knockdown cells in different phases of the cell cycle. (A) The percentage of cells in the G₁ phase significantly increased, whereas the percentages of cells in the S and G₂ phases significantly decreased in the shRNA-HIP1 group compared with shRNA-control group. (B) Statistical analysis of the percentage of cells in the shRNA-control and shRNA-HIP1 groups. *P<0.05. HIP1, huntingtin interacting protein 1; sh, short hairpin.

wound healing assay demonstrated that shRNA-control cells migrated at a faster rate compared with the shRNA-HIP1 cells (Fig. 3B). Similarly, the results of the Transwell assay demonstrated that shRNA-control cells migrated at a faster rate compared with the shRNA-HIP1 cells (Fig. 3C). The results of the invasion assay demonstrated that the invasive ability of shRNA-HIP1 cells significantly decreased compared with the shRNA-control cells (Fig. 3D).

HIP1 knockdown arrests EC109 cells in the G₁ phase of the cell cycle. Flow cytometric analysis demonstrated that the percentage of the shRNA-HIP1 group cells in the G₁ phase was significantly higher than the shRNA-control group (58.70±0.05% vs. 57.82±0.15%; P<0.05; Fig. 4A and B). Conversely, the percentages of the shRNA-HIP1 group cells in the S phase (38.44±0.05% vs. 37.76±0.04%; P>0.05) and G₂ phase (2.85±0.10% vs. 4.42±0.19%; P<0.05) were significantly lower than the shRNA-control group (Fig. 4A and B). Taken together, these results suggest that inhibiting HIP1 exerts an inhibitory effect on ESCC proliferation by inducing cells to enter the G₁ phase from the S phase.

Overexpression of HIP1 by lentivirus-delivered RNA interfering. The results of the present study demonstrated that HIP1 mRNA and protein expression levels were lower in Kyse30 cells compared with all other ESCC cell lines. Thus, to further investigate the underlying molecular mechanism of HIP1 in ESCC, Kyse30 cells were infected with a lentiviral vector to overexpress HIP1 expression. The infection efficiency of GFP in Kyse30 cells infected with OE-HIP1 was >80% after 3 days of infection, at a MOI of 20 (Fig. 5A). After 3 days, RT-qPCR and western blot analyses were performed to determine the overexpression efficiency, respectively. The results demonstrated that HIP1 mRNA and protein expressions levels were significantly promoted in cells transfected with OE-HIP1 compared with the OE-control and control groups (P<0.05; Fig. 5B and C). The successful establishment of HIP1 gene overexpression provided a useful tool for further investigating the function of HIP1 in ESCC cell lines.

Overexpression of HIP1 promotes ESCC cell proliferation, migration and invasion. To determine the effect of HIP1

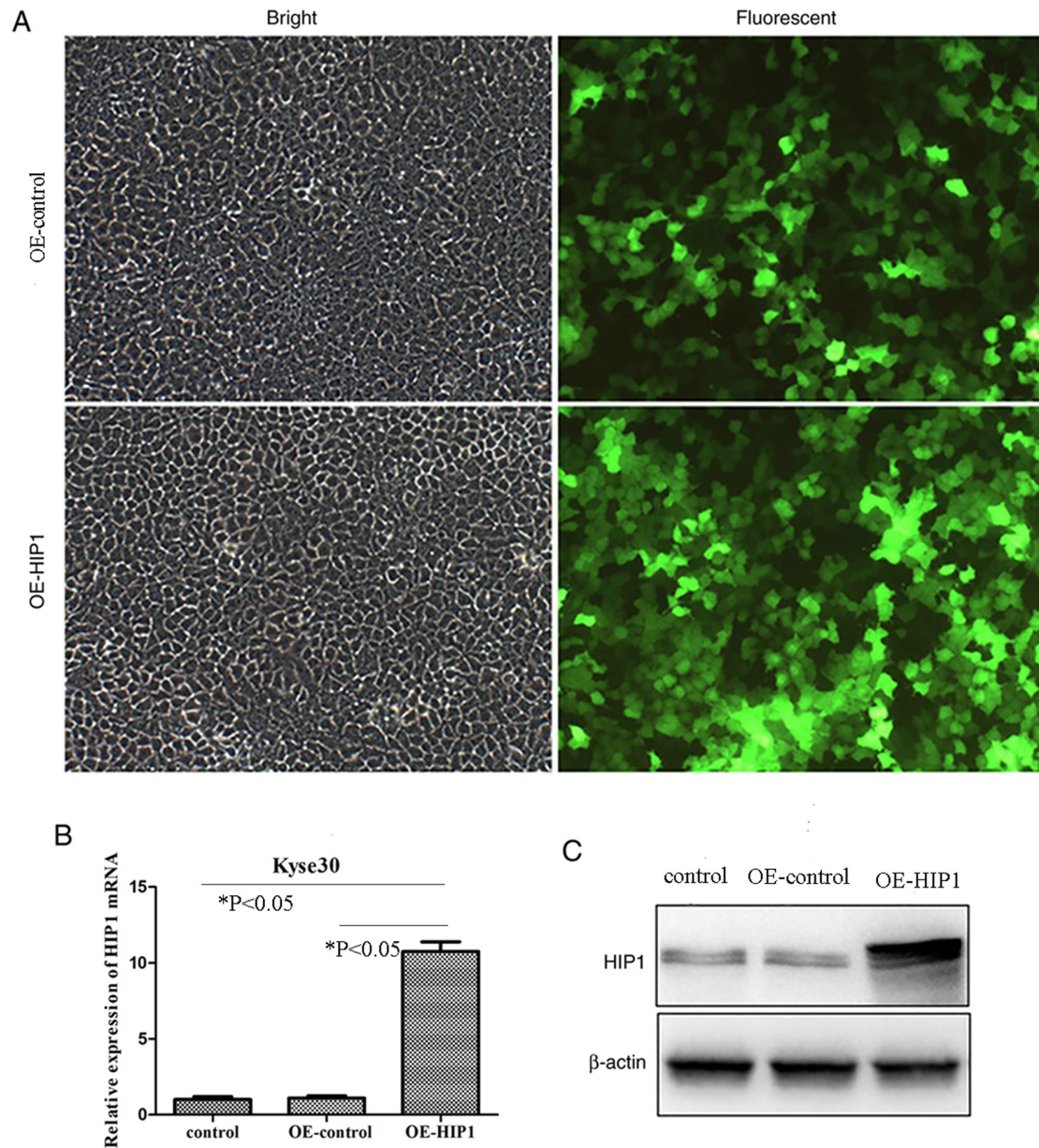


Figure 5. HIP1 expression is significantly overexpressed in Kyse30 cells transfected with OE-HIP1. (A) Micrograph of Kyse30 cells infected with OE-HIP1 for 3 days in bright and fluorescent fields (magnification, $\times 100$). The results demonstrated that $>80\%$ of Kyse30 cells infected with OE-HIP1 expressed green fluorescent protein. (B) Reverse transcription-quantitative PCR analysis demonstrated that HIP1 mRNA expression was significantly higher in Kyse30 cells transfected with OE-HIP1 compared the OE-control and control cells. (C) Western blot analysis demonstrated that HIP1 protein expression was remarkably higher in Kyse30 cells transfected with OE-HIP1 compared with the OE-control and control cells. $*P<0.05$. HIP1, huntingtin interacting protein 1; OE, overexpression.

overexpression on the biological behaviors of ESCC cells, overexpressed HIP1 cells were transfected into Kyse30 cells. The results of the MTT assay demonstrated that OE-HIP1 cells significantly promoted proliferation compared with the OE-control group ($P<0.01$; Fig. 6A). The results of the wound healing assay demonstrated that OE-HIP1 cells migrated at a faster rate compared with the OE-control group ($P<0.05$; Fig. 6B). Similarly, the results of the Transwell assay demonstrated that OE-HIP1 cells migrated at a faster rate compared with the OE-control group ($P<0.01$; Fig. 6C). The results of the invasion assay demonstrated that OE-HIP1 cells significantly promoted the invasive ability of Kyse30 cells ($P<0.01$; Fig. 6D). Collectively, these results suggest that overexpression

of HIP1 in Kyse30 cells may promote ESCC migration and invasion.

Overexpression of HIP1 induces Kyse30 cells to enter the S and G₂ phases from the G₁ phase. Flow cytometric analysis demonstrated that overexpression of HIP1 decreased the proportion of Kyse30 cells in the G₁ phase ($58.55\pm 0.48\%$ vs. $67.31\pm 0.29\%$; $P<0.05$), with concomitant increase in the S phase ($21.97\pm 0.18\%$ vs. $17.66\pm 0.20\%$; $P<0.05$) and G₂ phase ($19.48\pm 0.33\%$ vs. $15.04\pm 0.09\%$; $P<0.05$), compared with the OE-control cells (Fig. 7A and B). Taken together, these results suggest that overexpression of HIP1 may induce Kyse30 cells to enter the S and G₂ phases from the G₁ phase of the cell cycle.

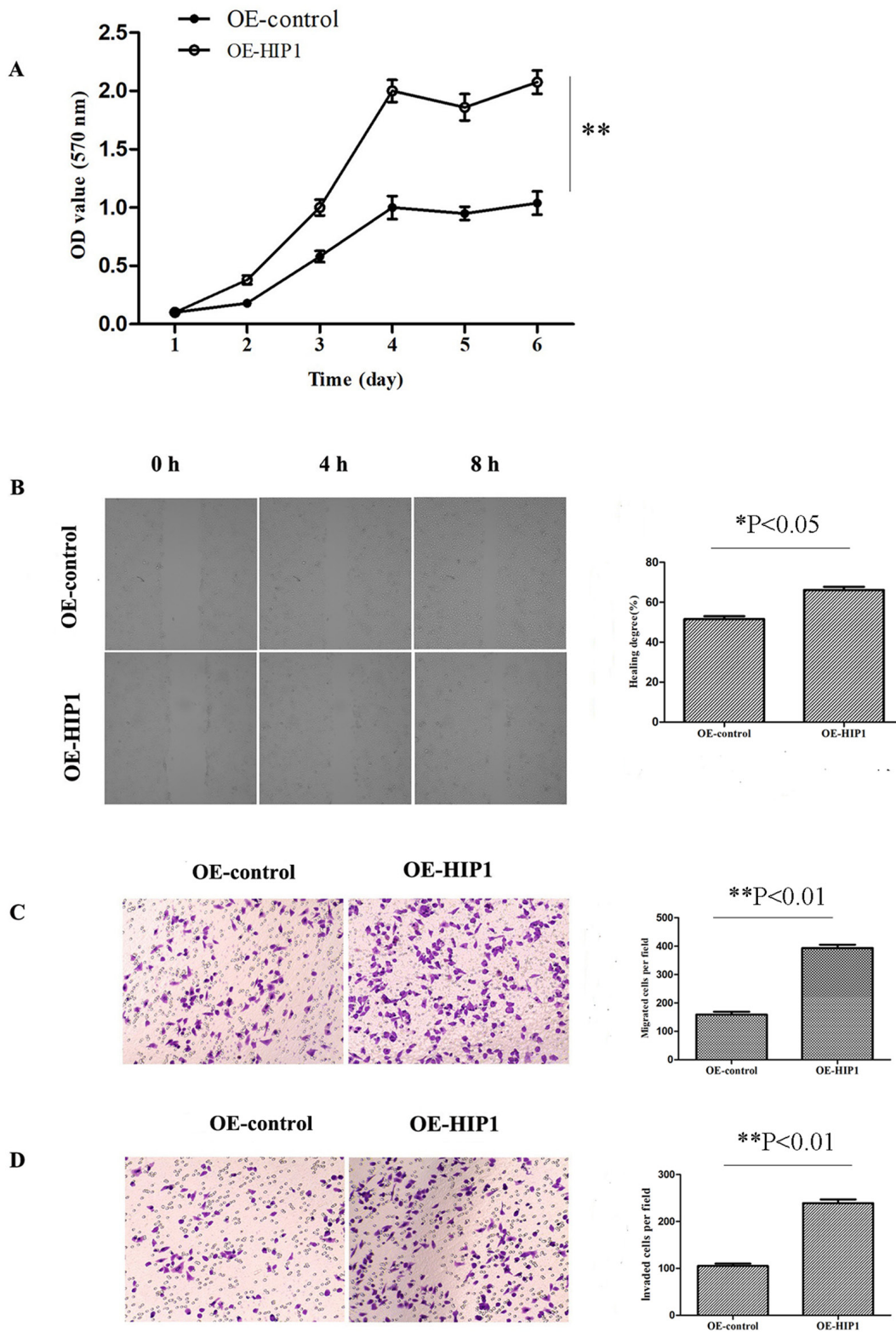


Figure 6. Overexpression of HIP1 significantly promotes esophageal squamous cell carcinoma cell proliferation, migration and invasion. (A) The results of the MTT assay demonstrated that OE-HIP1 promoted the proliferation of Kyse30 cells, in a time-dependent manner, compared with the OE-control group. The (B) wound healing and (C) Transwell migration assays demonstrated that overexpression of HIP1 promoted the migratory ability of Kyse30 cells (magnifications, x100 and x200, respectively). (D) The transwell invasion assay demonstrated that overexpression of HIP1 promoted the invasive ability of Kyse30 cells (magnification, x200). * $P < 0.05$, ** $P < 0.01$. HIP1, huntingtin interacting protein 1; OE, overexpression; OD, optical density.

Discussion

Efforts of molecular targeted drugs in tumor therapy are encouraging. However, there is a notable lag in the treatment

of esophageal cancer, thus it remains critical to identify novel biomarkers for early diagnosis and prognosis prediction. Previous studies have demonstrated the oncogenic function of HIP1, since its association with cancer was reported in

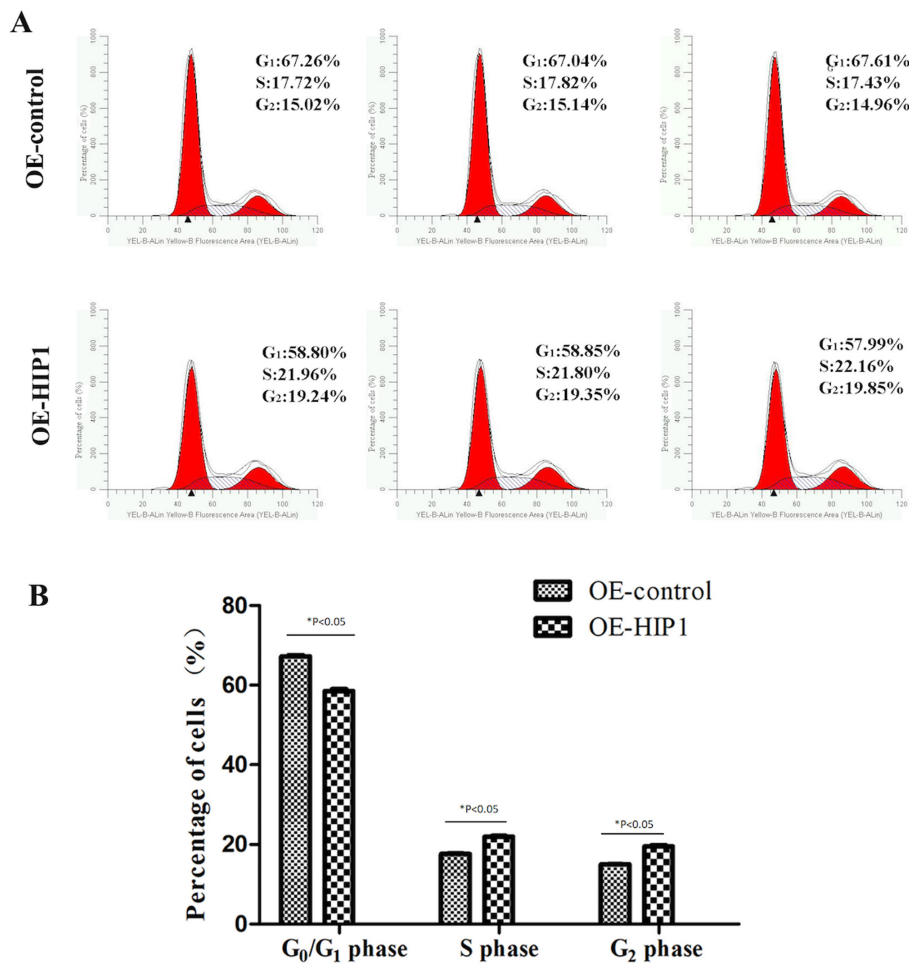


Figure 7. Percentage of HIP1 overexpressed Kyse30 cells in different phases of the cell cycle. (A) The percentage of cells in the G₁ phase significantly decreased, whereas the percentages of cells in the S and G₂ phases significantly increased in the OE-HIP1 group compared with the OE-control group. (B) Statistical analysis of the percentage of cells in the OE-control and OE-HIP1 groups. *P<0.05.

1997-1998 (18,19). These findings suggest that HIP1 may be a novel oncogene in tumors. However, the role and underlying molecular mechanism of HIP1 in ESCC have not yet been reported. Thus, the present study aimed to investigate the role of HIP1 in ESCC tumor progression.

IHC analysis was performed to detect HIP1 expression in 173 patients with ESCC. The results demonstrated that 89.6% (155/173) of patients with ESCC expressed HIP1. HIP1 mRNA and protein expression levels were also assessed via RT-qPCR and western blot analyses. The results demonstrated that HIP1 mRNA and protein expression levels were significantly higher in ESCC tissues compared with adjacent normal tissues. Wang *et al* (20) reported that elevated HIP1 expression is present in 67% of acute myeloid leukemia. By expanding the clinical sample size, the present study confirmed that patients with ESCC have elevated HIP1 mRNA and protein expression levels, suggesting that HIP1 expression is easily detectable in ESCC tissues. Hsu *et al* (21) demonstrated that low HIP1 expression is associated with clinical stage and inhibits the metastasis in non-small cell lung cancer. The results of the present study demonstrated that HIP1 expression was significantly associated with histological differentiation, TNM stage and lymph node metastasis in patients with ESCC. However, no significant association was observed between HIP1 expression

and smoking. Given that alcohol consumption was not included in the clinicopathological data, the association between HIP1 expression and alcohol consumption was not statistically analyzed in the present study. Thus, this will be investigated in prospective studies. In addition, whether there are other genes that cause abnormal HIP1 expression, or whether HIP1 is like the epidermal growth factor receptor gene in lung cancer remains the focus of future research. Taken together, the results of the present study suggest that HIP1 plays an important role in the occurrence and development of ESCC. However, whether HIP1 promotes or inhibits ESCC transfer needs to be confirmed through subsequent experiments.

The effect of different clinicopathological characteristics on the OS time of patients with ESCC was also investigated in the present study. Survival analysis demonstrated that differentiation, TNM stage and lymph node metastasis were all significantly associated with poor prognosis of ESCC. Similarly, Wang *et al* (20) reported that HIP1 expression is associated with poor prognosis in patients with acute myeloid leukemia. The results of the present study demonstrated that patients with high HIP1 expression had a significantly shorter survival time than patients with low HIP1 expression. Thus, it was hypothesized that HIP1 may be a transforming factor associated with poor prognosis in the development of ESCC.

Kaplan-Meier survival analysis demonstrated that differentiation, TNM stage, lymph node metastasis and HIP1 expression were all significantly associated with the prognosis of patients with ESCC. Notably, multivariate survival analysis demonstrated that differentiation, TNM stage and HIP1 expression were independent prognostic factors. Given that the TNM stage includes lymph node metastasis, only pathological grade, TNM stage and HIP1 expression were included in the multivariate survival analysis. The results demonstrated that the effect of HIP1 expression was more significant on the prognosis compared with differentiation and TNM stage, which may be closely associated with the importance of HIP1 on the prognosis of patients with ESCC. Collectively, these results suggest that HIP1 may be used as a potential independent biomarker to predict the prognosis of patients with ESCC.

The present study investigated the biological effects of inhibiting and overexpressing HIP1 on ESCC cell mobility *in vitro*. The results of the MTT, wound healing, and migration and invasion assays demonstrated that overexpressing HIP1 increased the proliferation, migration and invasion of Kyse30 cells, whereas silencing HIP1 decreased the proliferation, migration and invasion of EC109 cells. Flow cytometric analysis demonstrated that overexpression of HIP1 induced Kyse30 cells to enter the S and G₂ phases from the G₁ phase of the cell cycle, while HIP1 knockdown arrested EC109 cells in the G₁ phase. The results of the present study demonstrated that HIP1 affected cell cycle as well as cell migration and invasion; however, it is unclear whether these processes involve the same molecular mechanisms. It was speculated that when the esophagus becomes cancerous, HIP1 expression increases, which is accompanied by the proliferation of cancer cells and migration of cells into the S and G₂ phases. However, this speculation requires further investigation. Taken together, these results suggest that high HIP1 expression is closely associated with the development of esophageal cancer.

In conclusion, the results of the present study demonstrated that HIP1 expression was significantly higher in ESCC tissues compared with adjacent normal tissues. In addition, HIP1 expression was significantly associated with histological differentiation, TNM stage and lymph node metastasis. Notably, high HIP1 expression was associated with poor prognosis. Survival analysis demonstrated that HIP1 may be an independent predictor and potential target for patients with ESCC. The results also demonstrated that overexpressing HIP1 promoted ESCC cell proliferation *in vitro*, while suppressing HIP1 inhibited ESCC cell proliferation by regulating the cell cycle. However, further studies involving animal experiments and clinical trials are required to determine whether HIP1 is a clinical therapeutic target for ESCC.

Acknowledgements

Not applicable.

Funding

The present study was supported by the Air Force Medical University Tangdu Hospital Innovation and Development foundation (grant no. 2016JCYJ009).

Availability of data and materials

The datasets used and analyzed during the present study are available from the corresponding author upon reasonable request.

Authors' contributions

YaZ, ZZ and TJ designed the present study. YS, JX, XW and YoZ performed the experiments. MW and JZ analyzed the data, and YS, YaZ, ZZ and TJ prepared and revised the manuscript for important intellectual content. All authors have read and approved the final manuscript.

Ethics approval and consent to participate

The present study was approved by the Regional Ethics Committee for Clinical Research of the Air Force Military Medical University (Xi' an, China; approval no. TDLL-201712-22). Written informed consent was provided by all patients prior to the study start for use of their medical records and tissue specimens for research purposes.

Patient consent for publication

Not applicable.

Competing interests

The authors declare that they have no competing interests.

References

- Lee YT, Tan YJ and Oon CE: Molecular targeted therapy: Treating cancer with specificity. *Eur J Pharmacol* 834: 188-196, 2018.
- da Cunha Santos G, Shepherd FA and Tsao MS: EGFR mutations and lung cancer. *Annu Rev Pathol* 6: 49-69, 2011.
- Mahtani R, Holmes FA, Badve S, Caldera H, Coleman R, Mamounas E, Kalinsky K, Kittaneh M, Lower E, Pegram M, *et al*: A roundtable discussion of the breast cancer therapy expert group (BCTEG): Clinical developments and practice guidance on human epidermal growth factor receptor 2 (HER2)-positive breast cancer. *Clin Breast Cancer* 20: e251-e260, 2020.
- Zhang L, Wang H, Li W, Zhong J, Yu R, Huang X, Wang H, Tan Z, Wang J and Zhang Y: Pazopanib, a novel multi-kinase inhibitor, shows potent antitumor activity in colon cancer through PUMA-mediated apoptosis. *Oncotarget* 8: 3289-3303, 2017.
- Kalchman MA, Koide HB, McCutcheon K, Graham RK, Nichol K, Nishiyama K, Kazemi-Esfarjani P, Lynn FC, Wellington C, Metzler M, *et al*: HIP1, a human homologue of *S. cerevisiae* Sla2p, interacts with membrane-associated huntingtin in the brain. *Nat Genet* 16: 44-53, 1997.
- Waelter S, Scherzinger E, Hasenbank R, Nordhoff E, Lurz R, Goehler H, Gauss C, Sathasivam K, Bates GP, Lehrach H and Wanker EE: The huntingtin interacting protein HIP1 is a clathrin and alpha-adaptin-binding protein involved in receptor-mediated endocytosis. *Hum Mol Genet* 10: 1807-1817, 2001.
- Metzler M, Legendre-Guillemain V, Gan L, Chopra V, Kwok A, McPherson PS and Hayden MR: HIP1 functions in clathrin-mediated endocytosis through binding to clathrin and adaptor protein 2. *J Biol Chem* 276: 39271-39276, 2001.
- Gottfried I, Ehrlich M and Ashery U: HIP1 exhibits an early recruitment and a late stage function in the maturation of coated pits. *Cell Mol Life Sci* 66: 2897-2911, 2009.
- Bradley SV, Smith MR, Hyun TS, Lucas PC, Li L, Antonuk D, Joshi I, Jin F and Ross TS: Aberrant Huntingtin interacting protein 1 in lymphoid malignancies. *Cancer Res* 67: 8923-8931, 2007.

10. Marghalani S, Feller JK, Mahalingam M and Mirzabeigi M: Huntingtin interacting protein 1 as a histopathologic adjunct in the diagnosis of merkel cell carcinoma. *Int J Dermatol* 54: 640-647, 2015.
11. Rao DS, Hyun TS, Kumar PD, Mizukami IF, Rubin MA, Lucas PC, Sanda MG and Ross TS: Huntingtin-interacting protein 1 is over-expressed in prostate and colon cancer and is critical for cellular survival. *J Clin Invest* 110: 351-360, 2002.
12. Sun Y, Han Y, Wang X, Wang W, Wang X, Wen M, Xia J, Xing H, Li X and Zhang Z: Correlation of EGFR Del 19 with Fn14/JAK/STAT signaling molecules in non-small cell lung cancer. *Oncol Rep* 36: 1030-1040, 2016.
13. Zhao J, Zhou Y, Zhang Z, Tian F, Ma N, Liu T, Gu Z and Wang Y: Upregulated fascin1 in non-small cell lung cancer promotes the migration and invasiveness, but not proliferation. *Cancer Lett* 290: 238-247, 2010.
14. Wang WP, Sun Y, Lu Q, Zhao JB, Wang XJ, Chen Z, Ni YF, Wang JZ, Han Y, Zhang ZP, *et al*: Gankyrin promotes epithelial-mesenchymal transition and metastasis in NSCLC through forming a closed circle with IL-6/STAT3 and TGF- β /SMAD3 signaling pathway. *Oncotarget* 8: 5909-5923, 2017.
15. Liu T, Li WM, Wang WP, Sun Y, Ni YF, Xing H, Xia JH, Wang XJ, Zhang ZP and Li XF: Inhibiting CREPT reduces the proliferation and migration of non-small cell lung cancer cells by down-regulating cell cycle related protein. *Am J Transl Res* 8: 2097-2113, 2016.
16. Liang CC, Park AY and Guan JL: In vitro scratch assay: A convenient and inexpensive method for analysis of cell migration in vitro. *Nat Protoc* 2: 329-333, 2007.
17. Donohoe CL and Phillips AW: Cancer of the esophagus and esophagogastric junction: An 8th edition staging primer. *J Thorac Dis* 9: E282-E284, 2017.
18. Ross TS, Bernard OA, Berger R and Gilliland DG: Fusion of Huntingtin interacting protein 1 to platelet-derived growth factor beta receptor (PDGFbetaR) in chronic myelomonocytic leukemia with t(5;7)(q33;q11.2). *Blood* 91: 4419-4426, 1998.
19. Hong M, Kim RN, Song JY, Choi SJ, Oh E, Lira ME, Mao M, Takeuchi K, Han J, Kim J and Choi YL: HIP1-ALK, a novel fusion protein identified in lung adenocarcinoma. *J Thorac Oncol* 9: 419-422, 2014.
20. Wang J, Yu M, Guo Q, Ma Q, Hu C, Ma Z, Yin X, Li X, Wang Y, Pan H, *et al*: Prognostic significance of huntingtin interacting protein 1 expression on patients with acute myeloid leukemia. *Sci Rep* 7: 45960, 2017.
21. Hsu CY, Lin CH, Jan YH, Su CY, Yao YC, Cheng HC, Hsu TI, Wang PS, Su WP, Yang CJ, *et al*: Huntingtin-interacting protein-1 is an early-stage prognostic biomarker of lung adenocarcinoma and suppresses metastasis via Akt-mediated epithelial-mesenchymal transition. *Am J Respir Crit Care Med* 193: 869-880, 2016.



This work is licensed under a Creative Commons Attribution-NonCommercial-NoDerivatives 4.0 International (CC BY-NC-ND 4.0) License.